Journal of Alloys and Compounds 504 (2010) 211–216

Contents lists available at ScienceDirect

Journal of Alloys and Compounds

journal homepage: www.elsevier.com/locate/jallcom

Phase formation, microstructure and dielectric properties of $Sr_{0.53}Ba_{0.47}Nb_{2-x}Ta_xO_6$ ceramics

Zupei Yang[a,b,*], Rui Gu[a,b], Lingling Wei[a,b], Hongmei Ren[a,b]

[a] Key Laboratory for Macromolecular Science of Shaanxi Province, Xi'an, 710062, Shaanxi, PR China
[b] School of Chemistry and Materials Science, Shaanxi Normal University, Xi'an, 710062, Shaanxi, PR China

ARTICLE INFO

Article history:
Received 1 December 2009
Received in revised form 15 May 2010
Accepted 21 May 2010
Available online 31 May 2010

Keywords:
Ceramics
X-ray diffraction
Microstructure
Sintering

ABSTRACT

Ta^{5+} doped strontium barium niobate (SBN) ceramics were synthesized by conventional oxide-mixed method. The phase structure, microstructure and dielectric properties of the ceramics with different Ta^{5+} contents and sintering temperatures were investigated. The X-ray diffraction patterns show that pure tungsten bronze structure can be obtained in all the ceramics. The ceramics with high relative density and a uniform and fine-grained microstructure could be obtained at 1430 °C. The grain size of $Sr_{0.53}Ba_{0.47}Nb_{2-x}Ta_xO_6$ decreased with increasing the Ta^{5+} content. The relaxor behavior observed in SBNT ceramics should be attributed to a cationic disorder induced by B-site substitutions, which was proved by linear fitting of the modified Curie–Weiss law. All samples are proved to be relaxor ferroelectric. It is also found that Curie temperature T_c and maximum dielectric constant ε_m both decrease with increasing Ta^{5+} content.

1. Introduction

Strontium barium niobate $Sr_xBa_{1-x}Nb_2O_6$ (SBN) is a ferroelectric solid solution between $BaNb_2O_6$ (BN) and $SrNb_2O_6$ (SN), which is of tungsten bronze (TB) structure with a unit-cell formula of $[(A1)_2(A2)_4C_4][(B1)_2(B2)_8]_{30}$ [1,2]. In the structure of SBN, only five A-sites are occupied out of six and it results in a so-called unfilled structure that is responsible for charge disorder and relaxor behavior. It is reported that the SBN can be obtained in a wide composition ranges ($0.25 \le x \le 0.75$) [3]. This allows adjusting the Sr/Ba ratio to satisfy with the different requirements with appropriate physical and dielectric properties. SBN has received considerable attention as one type of lead-free electroceramics. Nowadays, SBN has been widely used in many practical applications such as electro-optic, pyroelectric, piezoelectric and photorefractive device because of its excellent pyroelectric and linear electro-optic coefficients [4–8].

In the TB structure, A type of cations occupy A1, A2 and C sites while B type of cations occupy the B1 and B2 octahedral sites [9]. In the formula, A1, A2, C and B are 15-, 12-, 9- and 6-fold coordinated sites in the crystal lattice structure. Generally, A1 and A2 sites can be filled by Na^+, K^+, Ca^{2+}, Sr^{2+}, Ba^{2+}, Pb^{2+}, and Bi^{3+}, etc., whereas B1 and B2 sites can be filled by W^{6+}, Nb^{5+}, and Ta^{5+}, the smallest interstice C is often empty, hence a formula is $A_6B_{10}O_{30}$ for the filled TB structure. Many physical and chemical properties may vary significantly by desired impurities doping or substituting [10,11]. For instance, alkali elements' doping on SBN showed a great increase in transition temperature and a decrease in dielectric loss [12]. Nishiwaki et al. found that rare earth elements (RE) and Li ions increased the transition temperature with decreasing the RE ionic ratio [15].

Until now, only a few researches were carried out on the aspect of doping SBN system such as transition temperature, dielectric properties and so on. The influence of doping on dielectric properties of SBN-based ceramics has seldom been studied in detail. In this work, the influences of Ta^{5+} content on the phase structure, density and dielectric properties of $Sr_{0.53}Ba_{0.47}Nb_2O_6$ ceramics were experimentally studied, and the diffuse phase transition of $Sr_{0.53}Ba_{0.47}Nb_{2-x}Ta_xO_6$ ceramics were investigated and discussed.

2. Experimental procedure

Conventional mixed-oxide method was used to prepare $Sr_{0.53}Ba_{0.47}Nb_{2-x}Ta_xO_6$ (x = 0.00, 0.05, 0.10, 0.15, 0.20, 0.25, 0.30, 0.35, 0.40) (abbreviated as SBNT) ceramics by using reagent-grade powders of $SrCO_3$ (99%), $BaCO_3$ (99%), Nb_2O_5 (99.5%) and Ta_2O_5 (99.99%). They were mixed by ball-milling in ethanol for 12 h using zirconia balls. The mixed powders were dried at 80 °C and calcined at 1250 °C for 4 h in air, respectively. Then the calcined powders were pressed into disks with a diameter of 15 mm under 100 MPa pressure using a solution of polyvinyl alcohol as binder. After a 500 °C binder burnout, the samples were sintered at 1350–1450 °C for 6 h in air, respectively. Silver paste was fired on both faces of the samples as electrodes.

The crystalline phase of the sintered ceramics was identified by X-ray diffraction (XRD, Model DMX-2550/PC, Rigaku, Japan) technique using Cu Kα radiation. The density of sintered samples was determined by the Archimedes method and the surface microstructures of the obtained ceramics were observed by scanning

* Corresponding author at: School of Chemistry and Materials Science, Shaanxi Normal University, Xi'an, 710062, Shaanxi, PR China. Tel.: +86 29 8531 0352; fax: +86 29 8530 7774.
E-mail address: yangzp@snnu.edu.cn (Z. Yang).

0925-8388/$ – see front matter © 2010 Elsevier B.V. All rights reserved.
doi:10.1016/j.jallcom.2010.05.093

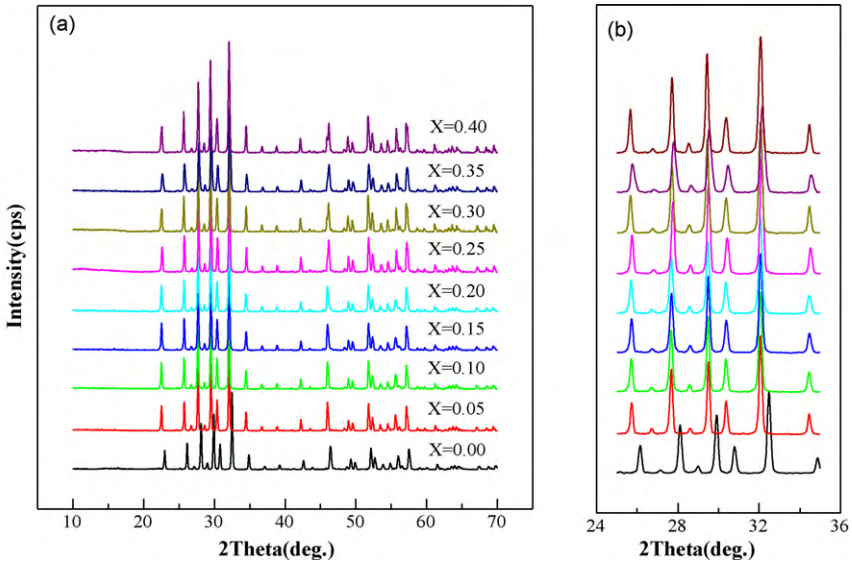

Fig. 1. XRD patterns of ceramics as a function of *x*.

electron microscopy (SEM, Model Quanta 200 FEI Company). The average grain size (d) was calculated by the following equation: $d = D/\sqrt{N}$ (μm), where D (μm) is the diameter of the circle drawn on the microstructure. The diameter of the circle drawn D is selected according to the grain sizes. N is the total number of the grains in the circle. N is calculated by the following equation: $N = P + 0.5Q$, where P is the number of complete grains in the circle; Q is the number of partial grains in the circle. Temperature dependence of dielectric properties was measured with an LCR meter (HP4294A) from room temperature to 300 °C at 1, 10, 100, 200 and 300 kHz.

3. Results and discussion

3.1. Phase structure

Fig. 1a shows the XRD patterns of the ceramics with different Ta^{5+} contents. Fig. 1b is the magnification of Fig. 1a in the range from 25 to 35 °C. In Fig. 1a, all ceramics are of single tungsten bronze (TB) structure phase and no second phase can be detected, which indicates that Ta^{5+} has diffused into the tungsten bronze structure lattice to form a solid solution. The diffraction peaks are indexed according to JCPDS73-0126. In tetragonal SBN, Nb^{5+} ions (radius 0.64 Å) occupy the B sites and form NbO_6 groups associated with six oxygen atoms. Taking the radii of doped Ta^{5+} (radius 0.64 Å) into account, the Ta^{5+} ion substitute for the Nb^{5+} ions and forms the TaO_6 groups. As shown in Fig. 1b, all the diffraction peaks of $Sr_{0.53}Ba_{0.47}Nb_{2-x}Ta_xO_6$ (x = 0.00, 0.05, 0.10, 0.15, 0.20, 0.25, 0.30, 0.35, 0.40) slowly shift to lower angle direction, which is due to the substitution of Nb^{5+}(0.069 nm) by Ta^{5+} (0.068 nm). It makes distortion of the unit cell in SBN ceramics.

3.2. Microstructure development and densification behavior

Fig. 2 shows the density of the $Sr_{0.53}Ba_{0.47}Nb_{2-x}Ta_xO_6$ ceramics with different x. It can be seen from Fig. 2a that the density increases with increasing x and reaches the maximum value of 5.29 g/cm^3 at x = 0.20, which was about 99.2% of the theoretical value. The relative density was calculated based on the theoretical density of SBN52 (5.33 g/cm^3) [14] which is close to the composition of interest. Further increasing x to 0.40 causes the decrease of density to 5.21 g/cm^3 (relative density 97.7%). The Ta^{5+} doped samples have higher density than undoped samples, which may due to the smaller grain size of the ceramics. The inset figure shows the density variation

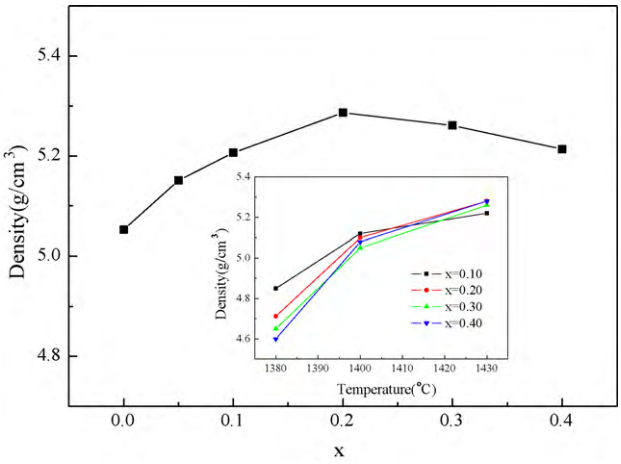

Fig. 2. Density of $Sr_{0.53}Ba_{0.47}Nb_{2-x}Ta_xO_6$ ceramics sintered at 1400 °C (inset figure: density of $Sr_{0.53}Ba_{0.47}Nb_{2-x}Ta_xO_6$ ceramics x = 0.1, 0.2, 0.3, 0.4 as a function of temperature).

of $Sr_{0.53}Ba_{0.47}Nb_{2-x}Ta_xO_6$ ceramics sintered at different temperatures. The density of sintered samples increases with increasing the sintering temperature. All samples sintered at 1430 °C for 6 h have the highest density. For the samples with high Ta^{5+} contents, the density increases sharply at lower temperatures and then increases slowly at higher temperatures.

Fig. 3 shows the SEM micrographs of the SBNT ceramics with different x and sintered at 1430 °C. As is shown in Fig. 3, all samples have uniform grains and clear crystalline boundaries. At the mean time, the grain growth behavior of the SBNT ceramics is restrained obviously by Ta^{5+} doping. The grain size decreases obviously with the addition of Ta^{5+}. The ceramics show large grains of 4–6 μm at x = 0.10. With increasing x, the grain sizes decrease. The microstructure with grain size ranging from 1.5 to 3 μm can be seen at x = 0.40. The results show that the grain growth is inhibited and the average grain sizes decrease as Ta^{5+} substituting for Nb^{5+}. The result reveals that a small amount of Ta^{5+} doped in SBN ceramics has an evident effect on grain size reduction as a grain growth inhibitor. It may be attributed to the segregation of some Ta^{5+} ions at grain bound-

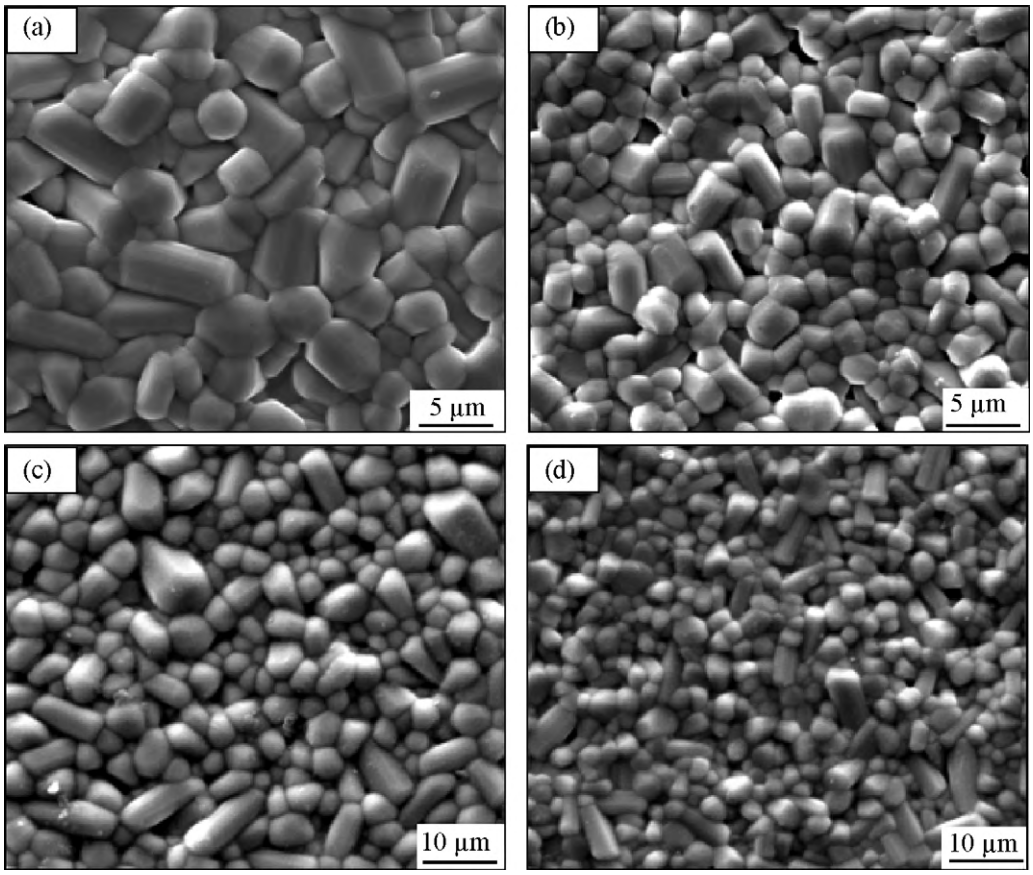

Fig. 3. SEM micrographs of $Sr_{0.53}Ba_{0.47}Nb_{2-x}Ta_xO_6$ ceramics: (a) $x = 0.10$; (b) $x = 0.20$; (c) $x = 0.30$; (d) $x = 0.40$ sintered at 1430 °C.

aries, thus preventing grain boundary movement during sintering and inhibiting grain growth.

Fig. 4 shows the microstructures of sample ($x = 0.10$) as a function of sintering temperature. As is shown in Fig. 4, with the sintering temperature increasing, the grain grows bigger, and the porosities become lower. The fine-grain and uniform microstructure in Fig. 4 is consistent with the density result in Fig. 2. A relative uniform grain size microstructure with fewer pores can be observed at 1400–1430 °C from Fig. 4c and d.

3.3. Dielectric properties

Fig. 5 shows the dielectric constant ε_r and dielectric loss tan δ for $Sr_{0.53}Ba_{0.47}Nb_{2-x}Ta_xO_6$ ceramics measured at 1 kHz and around room temperature as a function of x. It can be seen that with increasing x, ε_r increases firstly, reaches a maximum value of 2503 at $x = 0.10$, and then steeply decreases with further increasing x. On the other hand, tan δ decreases with increasing x. Finally, tan δ reaches a minimum value of 4.9×10^{-4} at $x = 0.40$.

Fig. 6 shows the dielectric constant ε_r for $Sr_{0.53}Ba_{0.47}Nb_{2-x}Ta_xO_6$ ceramics ($x = 0.05, 0.15, 0.25, 0.35$) around room temperature as a function of sintering temperature. It can be seen that with increasing the sintering temperature, ε_r for all sample increases slowly.

Fig. 7 shows the temperature dependence of the dielectric constant and dielectric loss with different frequencies for samples with different x ($x = 0.10, 0.15, 0.30, 0.40$). The figure shows the diffuse phase transition (DPT) characteristics (exhibiting a broad Curie peak in the phase transition range). With increasing the frequency, the dielectric constant at T_c shifted toward higher temperatures. $Sr_xBa_{1-x}Nb_2O_6$ ceramics are well-known DPT relaxor materials [15]. The relaxor behavior in SBNT ceramics should be attributed to a cationic disorder induced by B-site substitutions. In the solid solution of $Sr_{0.53}Ba_{0.47}Nb_{2-x}Ta_xO_6$, $Sr^{2+}$and Ba^{2+} ions occupy A1-sites and A2-sites, Nb^{5+} and Ta^{5+} ions occupy B-sites, therefore the ion disorder in the unit cell should be one of the reasons for the appearance of the frequency dispersion.

In order to further confirm the relaxor behavior of $Sr_{0.53}Ba_{0.47}Nb_{2-x}Ta_xO_6$ ceramics, quantitative characterizations have been done as described as follows.

A modified Curie–Weiss law is used to explain the dielectric behavior of complex ferroelectrics with diffuse phase transition. The formulation is as follows $1/\varepsilon - 1/\varepsilon_m = (T - T_m)\gamma/C$ [16]. In this formulation, γ is a constant which is used to express the diffuseness exponent of the phase transition. ε_m is the peak value of dielectric constant and T_m is the temperature at which ε_r reaches the maximum. When $\gamma = 1$, the materials with this type phase transition belong to normal ferroelectrics; when $1 < \gamma < 2$, the materials belong to relaxor ferroelectrics; when $\gamma = 2$, the materials belong to ideal relaxor ferroelectric. Fig. 8 shows $\ln[(\varepsilon_m/\varepsilon) - 1]$ as a function of $\ln(T - T_c)$ for ceramics measured at 1 kHz. A linear relationship is observed in all samples. It can be seen that γ of all ceramics is very close to 2, so the phase transition has a diffuse characteristic. Therefore, the material belongs to relaxor ferroelectric, which is in accordance with the results of Fig. 7.

Fig. 9 shows the variations of dielectric constant as a function of temperature (−100–150 °C) at 1 kHz for all different SBNT compositions. In all the samples, the dielectric constant increases with increasing temperature up to transition temperature (T_c) and then

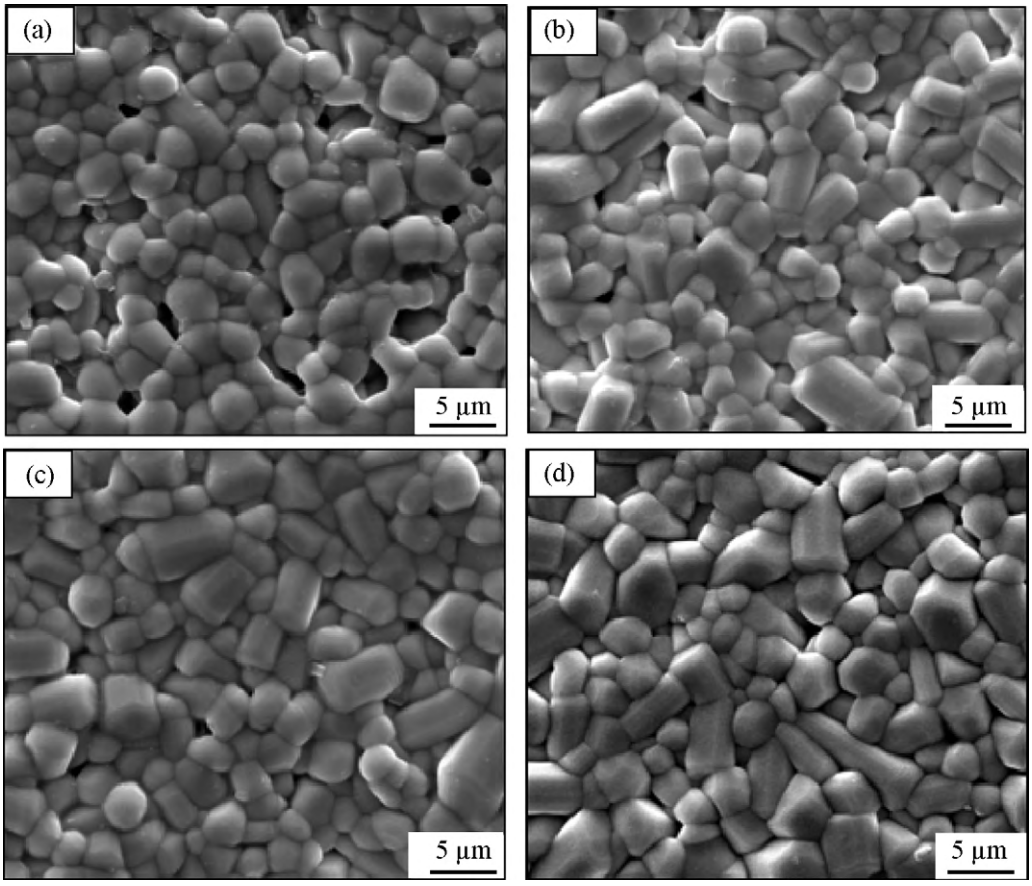

Fig. 4. SEM micrographs of $Sr_{0.53}Ba_{0.47}Nb_{2-x}Ta_xO_6$ ceramics ($x = 0.10$) sintered at different temperature (a) 1350 °C; (b) 1380 °C; (c) 1400 °C; (d) 1430 °C.

decreases with increasing temperature, which is normal behavior of ferroelectrics. From Fig. 9, it is found that T_c decreases with increasing x with a large fall in the maximum dielectric constant at T_c. Fig. 10a and b shows the transition temperature T_c and the maximum dielectric constant $\varepsilon_{m,}$ respectively. In all samples, the transition temperature T_c and the maximum dielectric constant ε_m decrease with increasing Ta^{5+}. Umakantham et al. reported that doping of K^+ and Na^+ in SBN leads to a filled structure without vacancies and raises the T_c implying stabilization of the structure [12]. The T_c decreases with Ta^{5+} concentration may be due to the structure vacancies which made by Ta^{5+}(0.068 nm) substituted for Nb^{5+} (0.069 nm). However, the rapid fall of maximum dielectric constant from 2461 to 1273 may be due to a decrease in crystallite size. In general, the decrease of crystallite size may decrease the dielectric constant. Ta doping in SBN has shown the decreasing crystallite size effect, which in turn may lead to the decrease of dielectric constant.

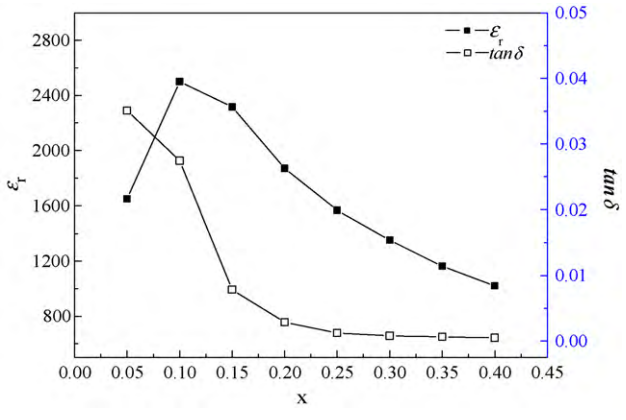

Fig. 5. Dielectric constant ε_r and dielectric loss tanδ for $Sr_{0.53}Ba_{0.47}Nb_{2-x}Ta_xO_6$ ceramics around room temperature as a function of x.

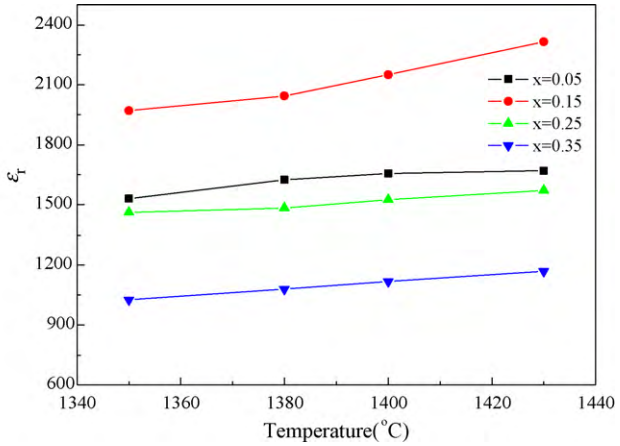

Fig. 6. Dielectric constant ε_r for $Sr_{0.53}Ba_{0.47}Nb_{2-x}Ta_xO_6$ ceramics ($x = 0.05, 0.15, 0.25, 0.35$) around room temperature as a function of temperature.

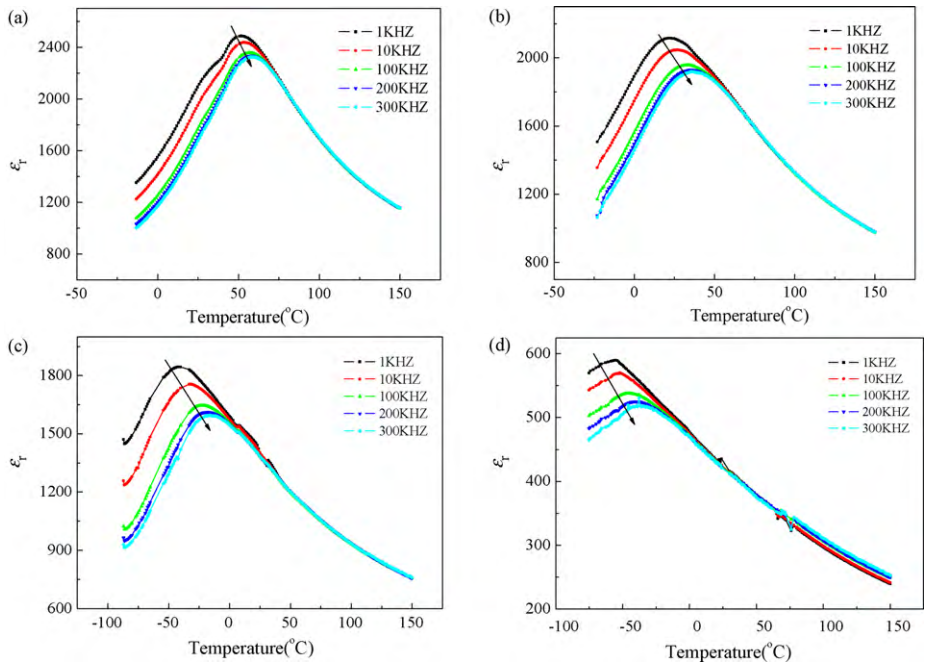

Fig. 7. Temperature dependence of dielectric constant and dielectric loss sintered at 1430 °C for 6 h: (a) $x = 0.10$ (b) $x = 0.15$ (c) $x = 0.30$ (d) $x = 0.40$.

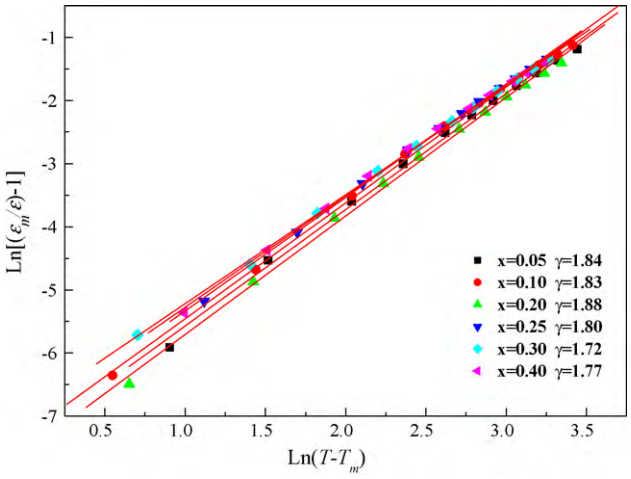

Fig. 8. $\ln[(\varepsilon_m/\varepsilon) - 1]$ as a function of $\ln(T - T_c)$ for ceramics at 1 kHz.

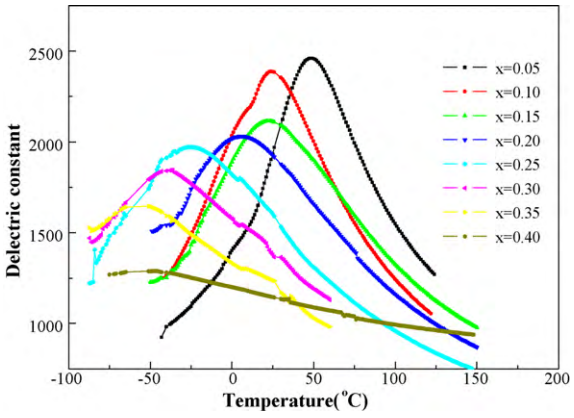

Fig. 9. Temperature dependent dielectric constant and curie of $Sr_{0.53}Ba_{0.47}Nb_{2-x}Ta_xO_6$ ceramics sintered at 1430 °C for various Ta^{5+} doping concentrations at 1 kHz frequency.

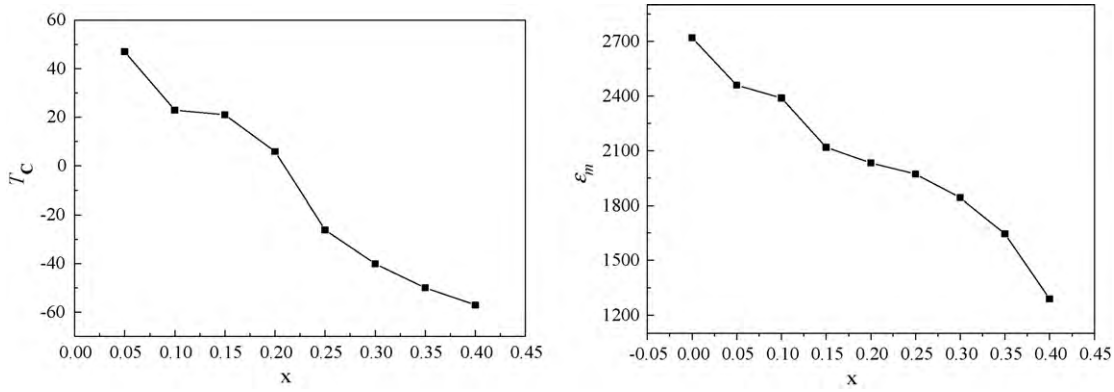

Fig. 10. (a and b) The ε_m and T_c of the $Sr_{0.53}Ba_{0.47}Nb_{2-x}Ta_xO_6$ ceramics sintered at 1430 °C for various Ta^{5+} doping concentrations at 1 kHz frequency.

4. Conclusions

Tungsten bronze structure $Sr_{0.53}Ba_{0.47}Nb_{2-x}Ta_xO_6$ ceramics with $x = 0.00$–0.40 were successfully prepared by solid state reaction method. The phase structure, density behavior, microstructure and dielectric properties of the SBNT ceramics were investigated. The XRD patterns show that the SBNT ceramics doped with $x = 0.00$–0.40 can form a single tungsten bronze (TB) structure solid solution. When the sintering temperature was 1430 °C, the ceramics with a near-theoretical density and a uniform and fine-grained microstructure were obtained. The SEM images indicate that the grain growth is restrained by Ta^{5+} doping. It was obvious that diffusive phase transition (DPT) took place in all these materials within the measuring temperatures. The relaxor behavior in SBNT ceramics should be attributed to cationic disorder induced by B-site substitutions. The relaxor ferroelectric characteristics are also proved by modified Curie–Weiss law with γ value varying between 1.7 and 1.9 at different frequencies. Therefore, the material belongs to relaxor ferroelectric. The transition temperature T_c and the maximum dielectric constant ε_m both decrease with Ta^{5+} increasing.

Acknowledgements

This work was supported by National Science Foundation of China (NSFC) (grant no. 20771070), Doctorial Program in China (grant no. 20070718004), Natural Science Research Program of Shaanxi Province (grant no. 2009JZ003). Fundamental Research Funds for the Central Universities.

References

[1] P.V. Lenzo, E.G. Spencer, A.A. Ballman, Appl. Phys. Lett. 11 (1967) 23–24.
[2] P.B. Jamieson, S.C. Abrahams, J.L. Bernstein, J. Chem. Phys. 48 (1968), 5048 ± 57.
[3] J.R. Carruthers, M. Grasso, J. Elecrochem. Soc. Solid State Sci. 117 (1970) 1426.
[4] B. Yang, F. Li, J.P. Han, X.J. Yi, H.L.W. Chan, H.C. Chen, W. Cao, J. Phys. D 37 (2004) 921–924.
[5] A.M. Glass, J. Appl. Phys. 40 (1969) 4699–4713.
[6] M. Kimura, T. Minamikawa, A. Ando, Y. Sakabe, Jpn. J. Appl. Phys. 36 (1997) 6051–6054.
[7] Z.X. Cheng, S.J. Zhang, G.Y. Zhou, J.H. Liu, J.R. Han, H.C. Chen, Mater. Res. Bull. 35 (2000) 1107–1112.
[8] B. Tribotte, J.M. Haussonne, G. Desgardin, J. Eur. Ceram. Soc. 19 (1999) 1105–1109.
[9] B. Jasmieson, S.C. Abrahams, J.L. Bernstein, J. Chem. Phys. 48 (1968) 5048–5057.
[10] A.Q. Jiang, G.H. Li, L.D. Zhang, J. Appl. Phys. 83 (1998) 4878–4883.
[11] Y. Wu, M.J. Forbess, S. Seraji, S.J. Limmer, T.P. Chou, G. Cao, Mater. Sci. Eng. B 86 (2001) 70–78.
[12] K. Umakantham, S. Narayana Murty, K. Sambasiva Rao, A. Bhanumathi, J. Mater. Sci. Lett. 6 (1987) 565.
[14] R.R. Neurgaonkar, W.K. Cory, J.R. Oliver, E.J. Sharp, G.L. Wood, G.L. Salamo, Ferroelectrics 142 (1993) 167.
[15] S. Nishiwaki, M. Kishi, J. Appl. Phys. 35 (1996) 5137.
[16] V.A. Isupov, Ferroelectrics 90 (1989) 113.